Supporting Information

Unraveling Structural Properties and Reactivity Trends of Cu-Ni Bimetallic Nanoalloy Catalyst for Biomass-Derived Levulinic Acid Hydrogenation

Pendem Saikiran,[a] Indranil Mondal,[a] Abhijit Shrotri,[b] Bolla Srinivasa Rao,[a] Nakka Lingaiah,[a] and John Mondal*[a]

[a]Inorganic & Physical Chemistry Division, CSIR-Indian Institute of Chemical Technology, Uppal Road, Hyderabad-500007, India

[b]Institute for Catalysis, Hokkaido University, Kita 21 Nishi 10, Kita-Ku, Sapporo, Japan, 001-0021

Characterization Techniques:

Powder X-ray diffraction (PXRD) patterns of different samples were recorded with a Rigaku Ultima IV X-ray diffractometer equipped with a semiconductor array detector (D/teX Ultra). High Resolution Transmission electron microscopy (HR-TEM) images were recorded in a JEOL JEM 2010 transmission electron microscope with operating voltage 200 Kv equipped with a FEG. Field emission scanning electron microscopic images of samples were obtained using a JEOL JSM 7400F field emission scanning electron microscope (FE-SEM). FT IR spectra of the samples were recorded using a Nicolet MAGNA-FT IR 750 Spectrometer Series II. Solid-state ^{13}C and ^{29}Si CP-MAS NMR studies were performed using a Bruker Avance III HD 400 MHz NMR spectrometer. Transmission electron microscope high-annular dark-field scanning (HAADF-STEM) and energy-dispersive X-ray mapping images were obtained with a TECNAI G2 F20 equipped with an EDX detector. X-ray photoelectron spectroscopy (XPS) was performed on an Omicron nanotech operated at 15 Kv and 20 Ma with a monochromatic Al Kα X-ray source. Quadrupole ion trap Mass Spectrometer equipped with Thermo Accela LC and Agilent 6890 GC system equipped with a flame ionization detector were used for analysis of catalytic reactions. The loading amounts of Cu and Ni were determined using an inductively coupled plasma optical emission spectrometer (ICP-OES, Icap-6500DUO, Thermo Fisher Scientific). The nature of the acid sites of the catalysts was examined by pyridine adsorbed FT-IR spectroscopy (Carry 660, Agilent Technologies). The experiments were performed in situ using a purpose-made IR cell connected to a vacuum adsorption setup. In a typical method, the reduced samples were pressed into self-supporting wafers (density 40 mg cm^{-3}) at a pressure of 10^5 Pa. Subsequently, the wafers were transferred into the IR cell and were pre-treated in N_2 flow by heating at a rate of 10ºC min^{-1} up to 400ºC for 1 h. After cooling down to 150ºC, the spectrum was collected in the drift mode. The sample was then exposed to pyridine until surface saturation in successive pulse injections at 150 ºC and subsequently the sample was purged for 30 min in N_2 flow before

recording the spectrum. The drift spectra after pyridine adsorption were subtracted from the spectra of the untreated catalyst to obtain the vibrational bands owing to pyridine acid site interaction. The H_2-TPR analysis was carried out in a quartz micro-reactor interfaced to a gas chromatograph (GC) equipped with a thermal conductivity detector (TCD) unit. Prior to TPR analysis, the catalyst was degassed at 300ºC in helium gas for 30 min and then cooled to room temperature. The helium gas was switched to 4.97% H_2 in argon with a flow rate of 30 mL min^{-1} and the temperature was increased to 900 ºC at a ramping rate of 5 ºC min^{-1}.

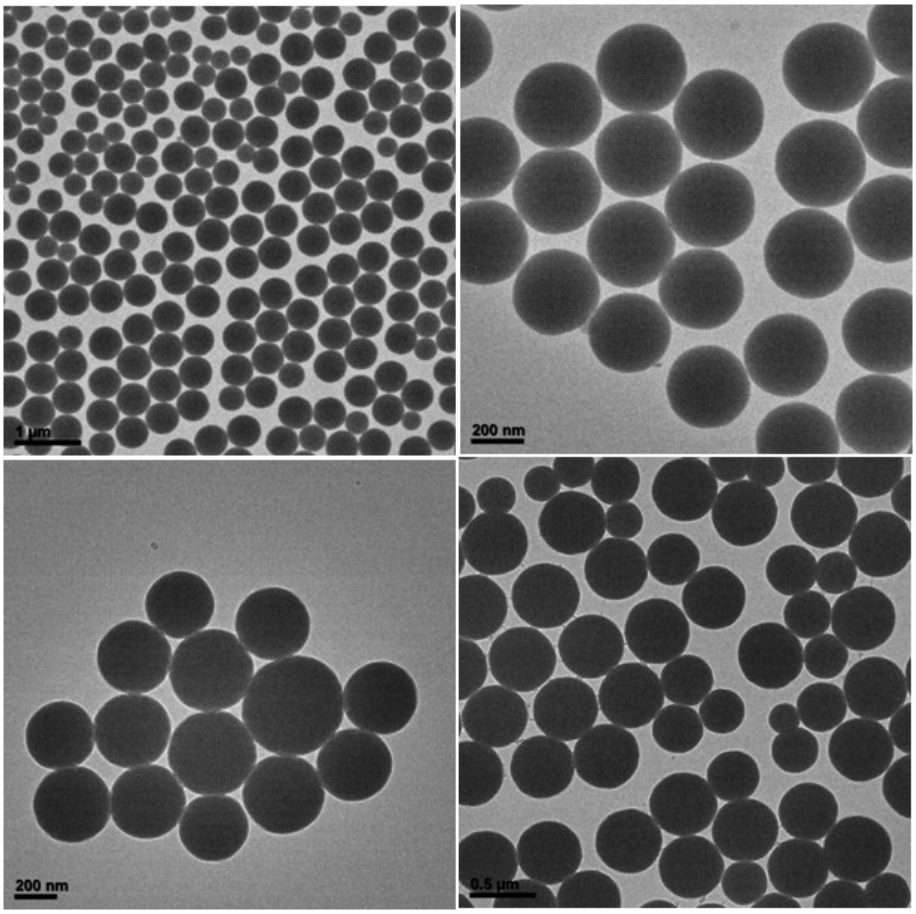

Figure S1: TEM images of the -NH_2 functionalized SiO_2 nanopshere.

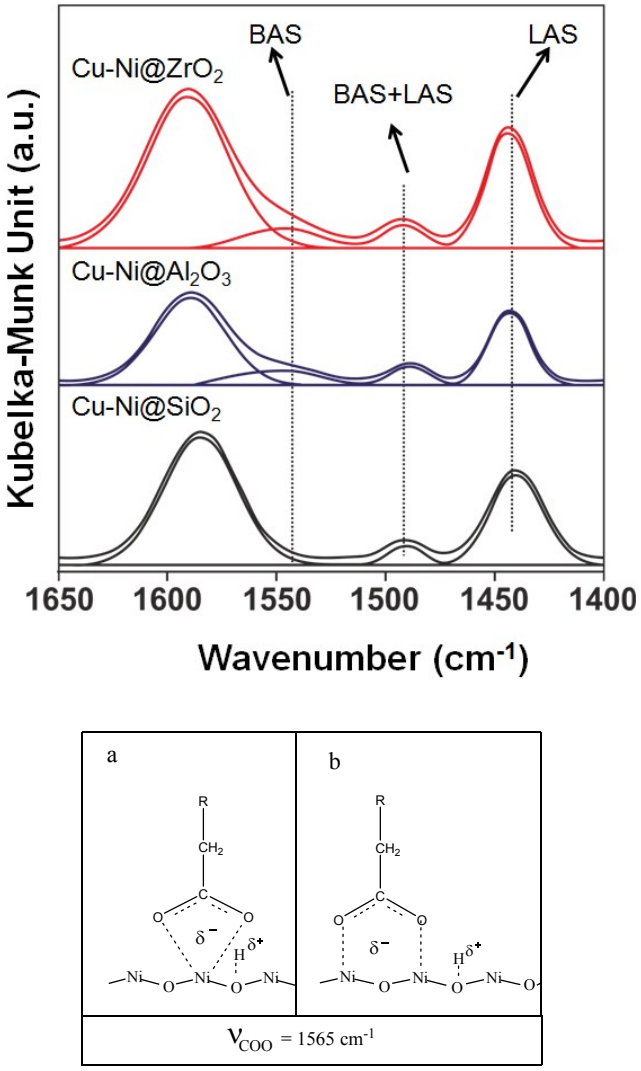

Figure S2: Pyridine adsorbed drift spectra of Cu-Ni@ZrO_2, Cu-Ni@Al_2O_3 and Cu-Ni@SiO_2 catalysts, respectively.

Table S1: Inductively coupled plasma optical emission spectroscopy (ICP OES) elemental analysis results of the bimetallic Cu-Ni nanoalloy.

Catalyst	Cu-content ($mmolg^{-1}$)	Ni-content ($mmolg^{-1}$)
CuNi@SiO_2-**A** (fresh)	0.00571	0.00032
CuNi@SiO_2-**B** (fresh)	0.00347	0.00191
CuNi@SiO_2-**C** (fresh)	0.00271	0.0028
CuNi@SiO_2-**A** (spent)	0.00535	0.00031
CuNi@SiO_2-**B** (spent)	0.00301	0.00165
CuNi@SiO_2-**C** (spent)	0.00213	0.0023

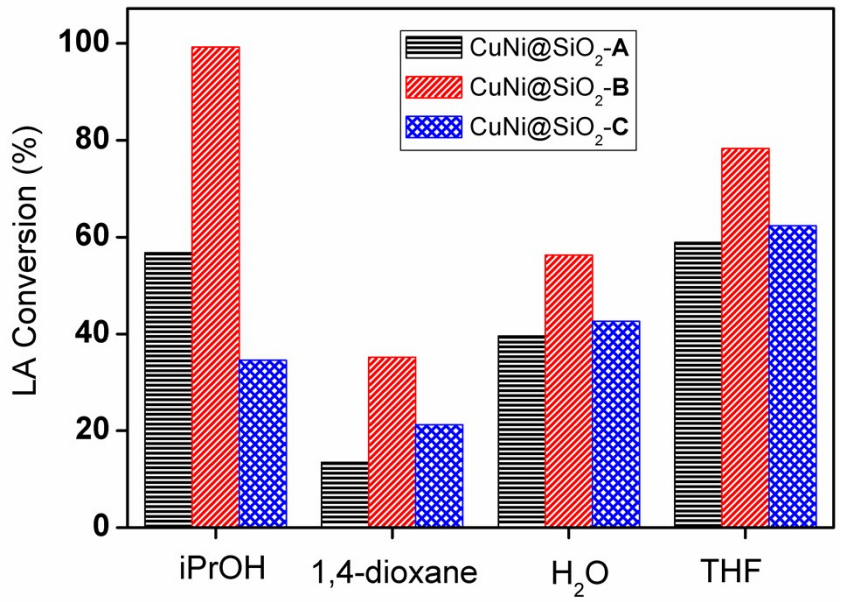

Figure S3: GVL yields as a function of the various solvent used in levulinic acid hydrogenation using CuNi@SiO_2-**B** catalyst. Experimental conditions: 0.2 mL levulinic acid (2 mmol), Temperature (120ºC), H_2 pressure (40 bar), Time (13 h), iPrOH (40 mL).

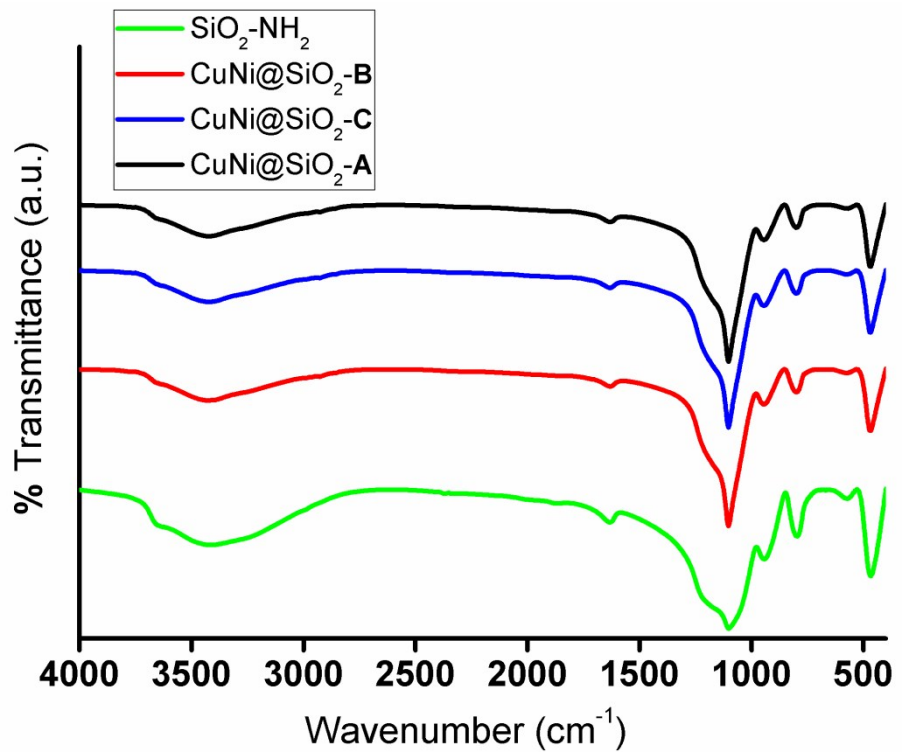

Figure S4: FT-IR spectra of all CuNi@SiO_2 materials.

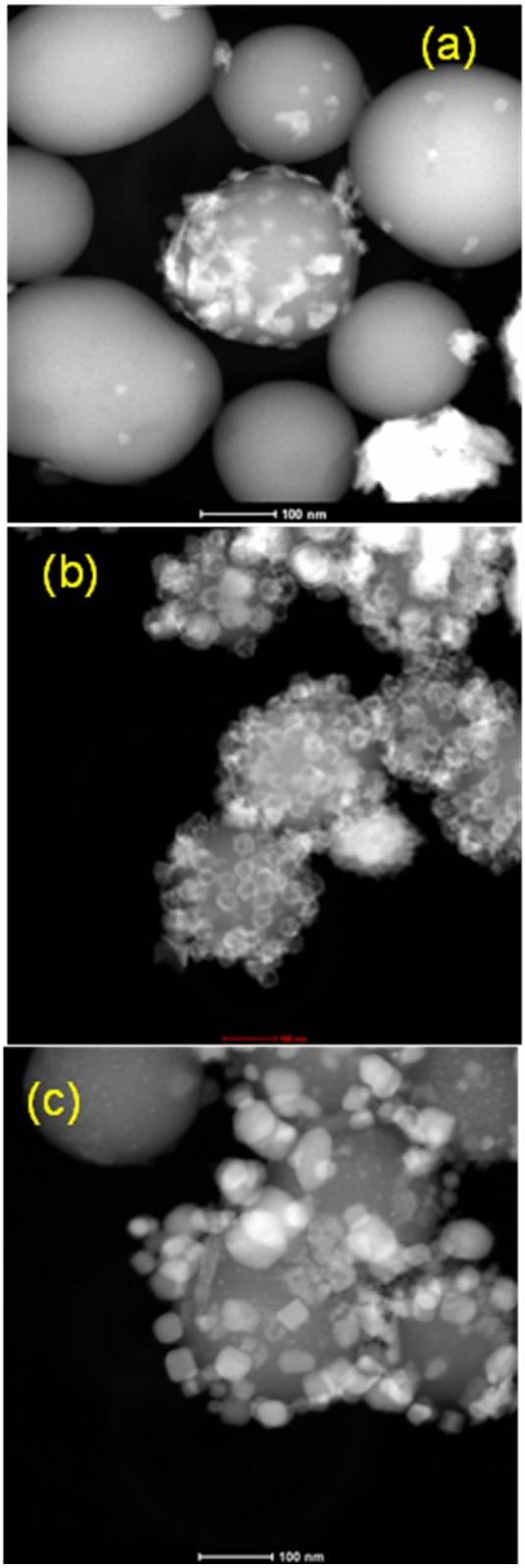

Figure S5: HAADF-STEM images of (a) CuNi@SiO_2-**A**, (b) CuNi@SiO_2-**B** and (c) CuNi@SiO_2-**C**, respectively.

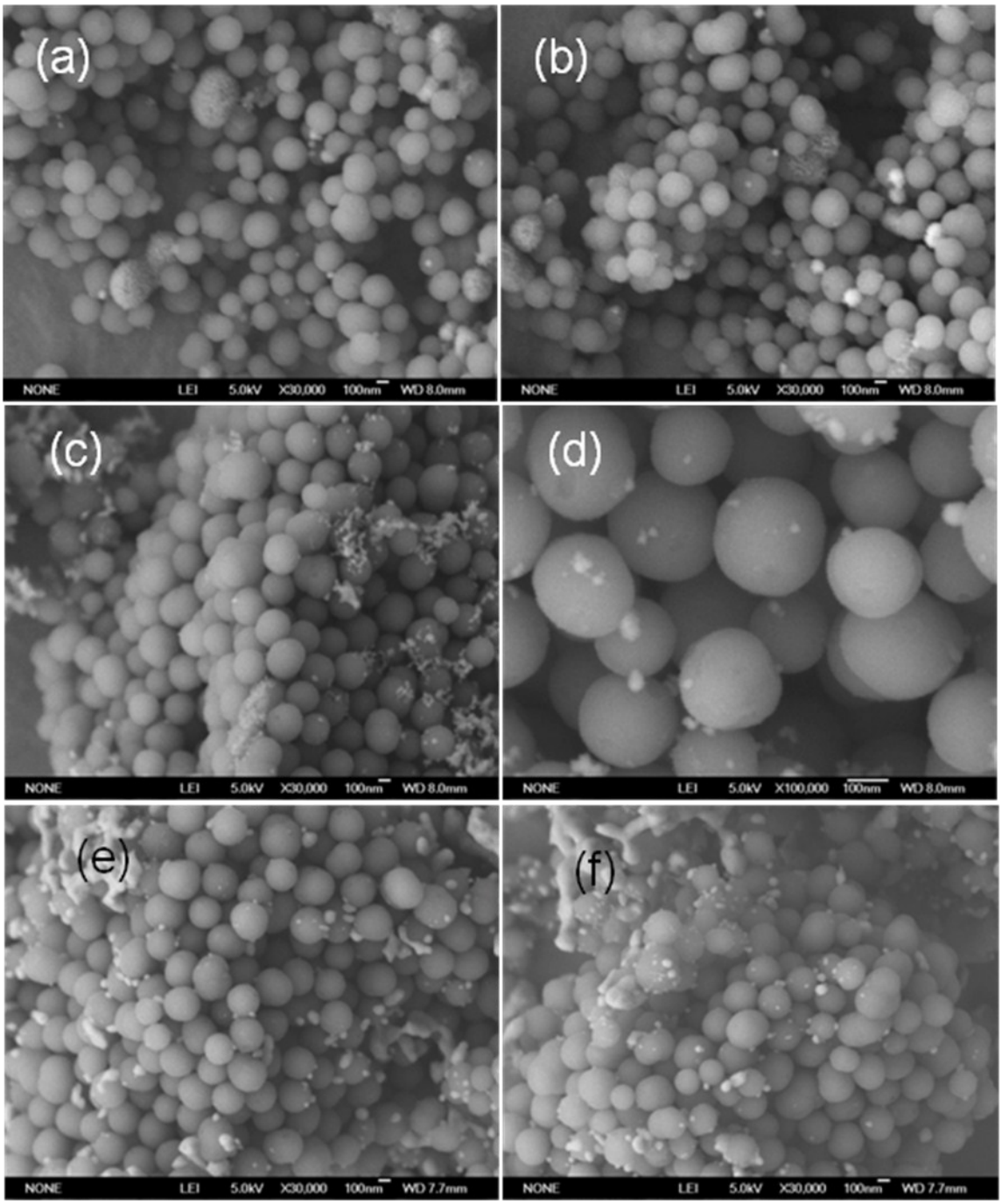

Figure S6: FE-SEM images of (a, b) CuNi@SiO_2-**A**, (c, d) CuNi@SiO_2-**B** and (e, f) CuNi@SiO_2-**C**, respectively.

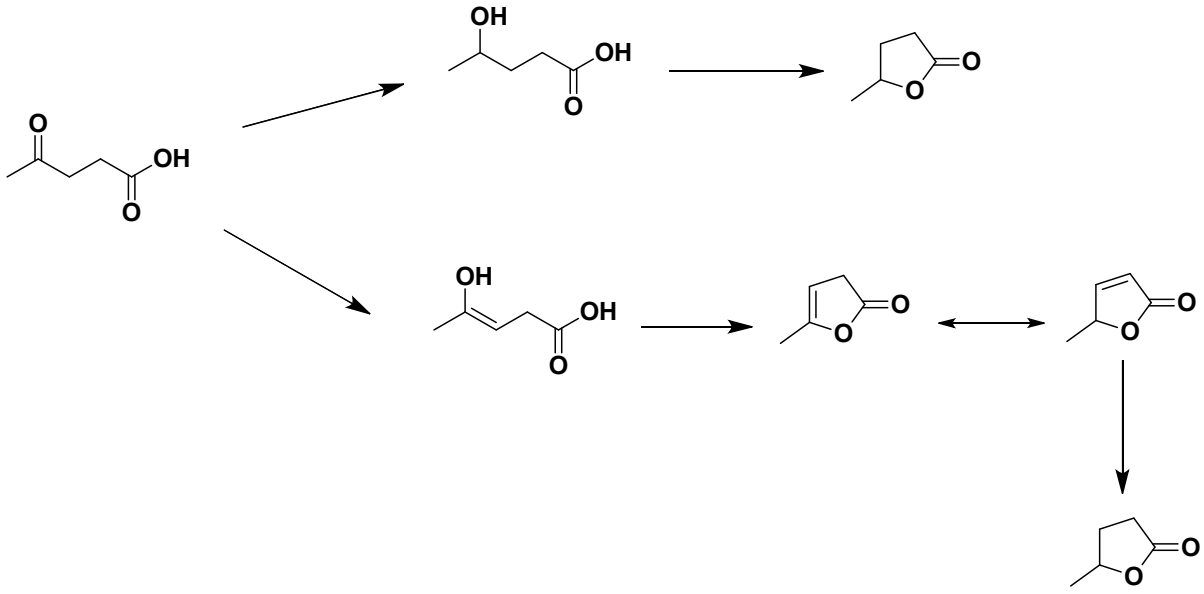

Figure S7: Proposed mechanistic pathway for LA hydrogenation to GVL.

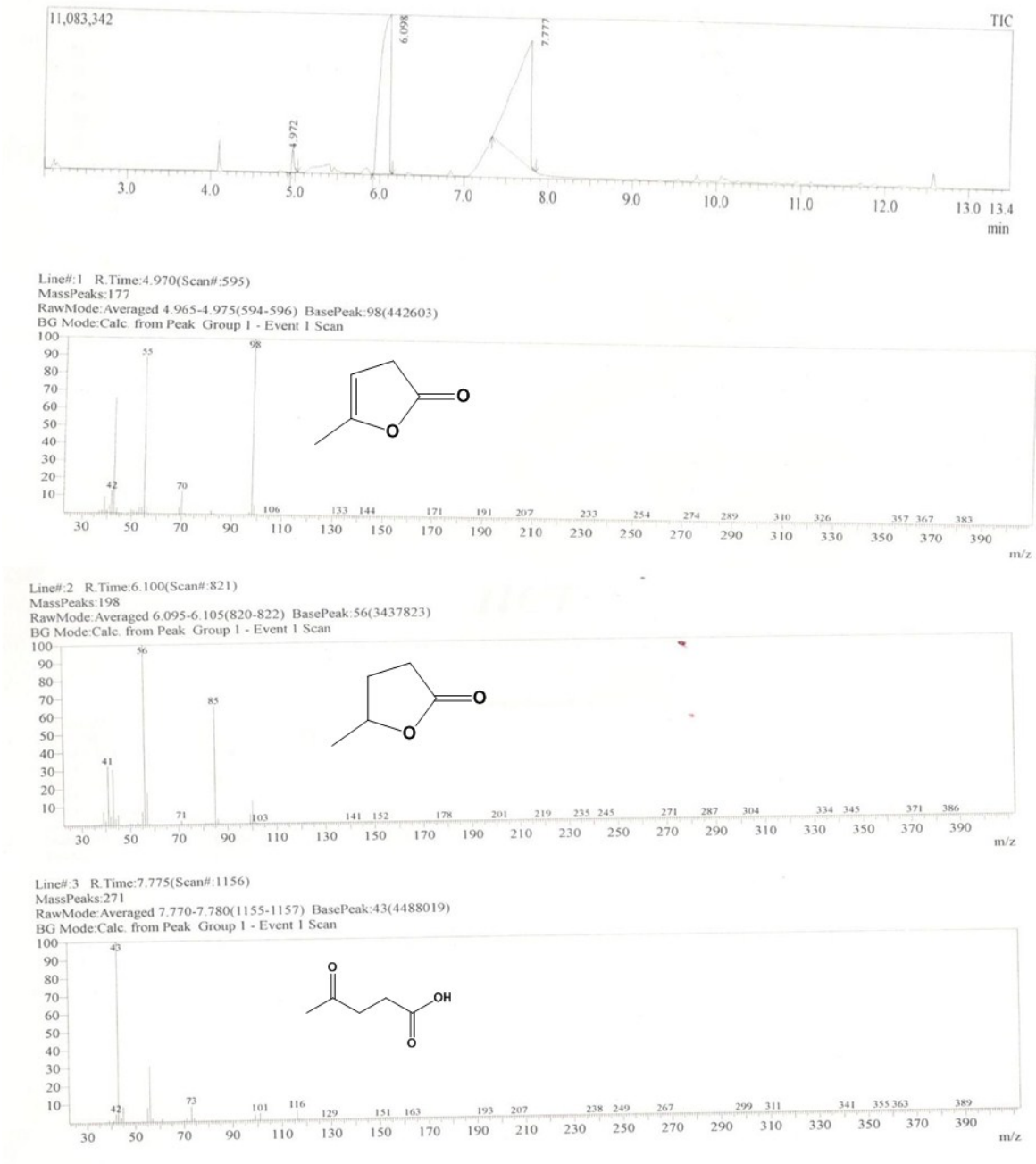

Figure S8: Progress of the catalytic LA to GVL hydrogenation by GC-MS analysis.